ISSN: 1314-6246 Brown *et al.* *J. BioSci. Biotech.* **2014**, 3(1): 49-60.

RESEARCH ARTICLE

An *in silico* analysis of the glutamate dehydrogenases of *Teladorsagia circumcincta* and *Haemonchus contortus*

Simon Brown [1,2]
Noorzaid Muhamad [3]
Lisa R. Walker [4]
Kevin C. Pedley [4]
David C. Simcock [1,4,5]

Authors' addresses:
[1] Deviot Institute, Deviot, Tasmania 7275, Australia.
[2] School of Human Life Sciences, University of Tasmania, Locked Bag 1320, Launceston, Tasmania 7250, Australia.
[3] University Kuala Lumpur, Royal College of Medicine Perak, 3 Greentown Road, 30450 Ipoh, Perak, Malaysia.
[4] Institute of Food, Nutrition and Human Health, Massey University, Private Bag 11222, Palmerston North, New Zealand.
[5] Faculty of Medicine, Health and Molecular Sciences, James Cook University, Cairns, Queensland 4870, Australia.

Correspondence:
Simon Brown
School of Human Life Sciences, University of Tasmania, Locked Bag 1320, Launceston, Tasmania 7250, Australia.
Tel.: +61 3 63245400
e-mail: Simon.Brown@deviotinstitute.org

Article info:
Received: 19 October 2013
Accepted: 29 November 2013

ABSTRACT

Nematode glutamate dehydrogenase (GDH) amino acid sequences are very highly conserved (68-99% identity) and are also very similar to those of the bovine and human enzymes (54-60% identity). The residues involved in binding nucleotides or substrates are completely conserved and tend to be located in highly conserved regions of the sequence. Based on the strong homology between the bovine, *Teladorsagia circumcincta* and *Haemonchus contortus* GDH sequences, models of the structure of the *T. circumcincta* and *H. contortus* monomers were constructed. The structure of the *T. circumcincta* monomer obtained using SWISS-MODEL was very similar to that of the bovine enzyme monomer and the backbone of the polypetide deviated very little from that of the bovine enzyme monomer. Despite the sequence differences between the bovine and *T. circumcincta* enzymes, the relative positions and orientations of the residues involved in ligand binding were very similar. The reported K_m for $NADP^+$ of *T. circumcincta* is about 35 and times that of the bovine enzyme, whereas the K_ms of the two enzymes for glutamate, α-ketoglutarate and NAD(P)H are much more similar. The residue corresponding to S267 of the bovine enzyme is involved in binding the 2′-phosphate of $NADP^+$ and is replaced in the *T. circumcincta* and *H. contortus* sequences by a tryptophan. The partial occlusion of the NAD(P)-binding site by the tryptophan sidechain and the loss of at least one potential H-bond provided by the serine may explain the lower affinity of the *T. circumcincta* for $NADP^+$.

Key words: glutamate dehydrogenase, structure, *Teladorsagia circumcincta*, parasite, nematode

Introduction

Teladorsagia circumcincta and *Haemonchus contortus* are common nematode parasites of sheep. In some regions the burden of parasitism by these species and their growing resistance to current anthelmintics has compromised the viability of sheep farming (Waller et al., 1996; van Wyk et al., 1997), but the welfare of the sheep is at risk without reliable control of the parasite burden. These, and other considerations, have motivated a search for new targets for anthelmintics.

One target that has been suggested (Umair et al., 2011) is glutamate dehydrogenase (GDH, E.C. 1.4.1.3), which catalyses the reversible oxidative deamination of glutamate to α-ketoglutarate using either NAD^+ or $NADP^+$ as the electron acceptor. The enzyme represents an important link between the tricarboxylic acid cycle and amino acid metabolism and has been extensively studied in mammals (Plaitakis & Zaganas, 2001; Owen et al., 2002; Newsholme et al., 2003; Frigerio et al., 2008), plants (Mayashita & Good, 2008), fungi (Marzluf, 1981) and bacteria (Hudson & Daniel, 1993), but nematode GDHs have received relatively little attention.

RESEARCH ARTICLE

The suggestion that GDH might be a target for anthelmintics was based on undefined differences in amino acid sequence between the nematode and host enzymes and on their kinetic characteristics (Umair et al., 2011). Such suggestions are not unique. For example, it has been suggested that the GDH of *Plasmodium* spp. might be a target for antimalarial therapy (Werner et al., 2005). *Plasmodium falciparum* has three *gdh* genes, but it has been demonstrated that it can survive without GDH a (Storm et al., 2011), whereas *Caenorhabditis elegans* has only one on chromosome 4. As we show, the *P. falciparum* enzyme is very different from that of either *T. circumcincta* or *H. contortus* and the lifestyles of the parasites are also dissimilar.

The three most significant features of the kinetic properties of the *T. circumcincta* GDH (*Tc*GDH) are (i) that it is active with either NAD(H) or NADP(H) (Muhamad et al., 2011), (ii) that the K_ms for the dinucleotides tend to be greater for the *Tc*GDH than for the bovine enzyme (*Bt*GDH) (Frieden, 1959; Engel & Dalziel, 1969; Rife & Cleland, 1980; McCarthy & Tipton, 1985), and (iii) the $K_m(NADP^+)$: $K_m(NAD^+)$ ratio is much greater for the *Tc*GDH than is the case for *Bt*GDH (Frieden, 1959; Engel & Dalziel, 1969; Rife & Cleland, 1980; McCarthy & Tipton, 1985), although the kinetics of the latter are known to be very complex. That the enzyme is able to use both NAD(H) and NADP(H) prompts the suggestion that it might have more in common with mammalian enzymes, which behave similarly (Rife & Cleland, 1980; McCarthy & Tipton, 1985), rather than the plant, bacterial or *Plasmodium* spp. enzymes, which tend exhibit specificity for either NAD(H) or NADP(H) (Gore, 1981; Storm et al., 2011). The high ratio of $K_m(NADP^+)$:$K_m(NAD^+)$ reported for *Tc*GDH is quite unlike *Bt*GDH, for example, for which the ratio is less than 1 (Frieden, 1959; Engel & Dalziel, 1969; Rife & Cleland, 1980; McCarthy & Tipton, 1985) and the difference appears to result from the very high K_m for $NADP^+$ reported for the *Tc*GDH (Muhamad et al., 2011; Umair et al., 2011). If the *H. contortus* GDH (*Hc*GDH) has a similarly high K_m for $NADP^+$, it might explain the report by Rhodes and Ferguson (1973) that this enzyme could utilise only NAD(H). From these observations, we infer that there might be some significant structural difference between *Tc*GDH and both *Hc*GDH and *Bt*GDH.

There has been no consideration of the structure of the nematode GDH, other than in a very preliminary form based on a partial *T. circumcincta* sequence (Green et al., 2004). In part this is due to the difficulty of obtaining sufficient nematodes from which to purify the enzyme. However, cDNA sequences of both *Hc*GDH and *Tc*GDH have been reported (Skuce et al., 1999; Umair et al., 2011) and the latter has been expressed in *Escherichia coli*. This recombinant *Tc*GDH (r*Tc*GDH) appears to behave almost identically to the *Tc*GDH in crude homogenates (Muhamad et al., 2011). Curiously, the specific activity of the r*Tc*GDH is only about 4 times that of the enzyme in crude homogenates (Muhamad et al., 2011). We infer from this that either *Tc*GDH is about 25% of the protein in *T. circumcincta*, which seems improbable, or that the r*Tc*GDH was adversely affected by the six-histidine tag engineered into it, the expression in *E. coli* or the purification procedure. However, Kim et al. (2003) applied a very similar strategy to *Bt*GDH and showed that the recombinant and the native enzyme had very similar kinetics, so the problem presumably lies elsewhere. Until this, and several others, issues are resolved, there is little point in attempting to determine the structure of the r*Tc*GDH, but the sequence of *Tc*GDH can provide some insight into the structural properties of the enzyme.

Here we report on the properties of the best of the models we have constructed using the *Tc*GDH and *Hc*GDH sequences and crystal structures of the homologous *Bt*GDH. These models provide a possible explanation for the very high $K_m(NADP^+)$ of *Tc*GDH, but do not explain the lack of activity of *Hc*GDH with $NADP^+$.

Materials and Methods

Glutamate dehydrogenase amino acid sequences were obtained from GenBank for *Caenorhabditis elegans* (NP_502267.1), *C. briggsae* (XP_002633432.1), *C. brenneri* (EGT40056.1), *C. remanei* (XP_003100701.1), *Ascaris suum* (ADY42913.1), *Brugia malayi* (XP_001893113.1), *H. contortus* (AAC19750.1), *Neospora caninum* (CBZ49515.1), *Plasmodium falciparum* (XP_001348337.1), *Toxoplasma gondii* (XP_002370120.1) and *T. circumcincta* (AEO44571.1). The crystal structures of *Bt*GDH (1HWY, 1HWZ and 3MW9), *P. falciparum* (2BMA) and human GDH (1L1F) were obtained from the Protein Databank (http://www.pdb.org/pdb/home/home.do) and the sequences used in the analysis are those of the crystals in order to maintain consistency between the sequence and structure analyses.

Sequences were aligned with ClustalX (Thompson et al., 1997) using the Gonnet substitution matrix, a gap opening penalty of 10 and a gap extension penalty of 0.2.

RESEARCH ARTICLE

The mutability of the sequences was quantified at position i in the alignment using

$$M_i = \frac{1}{(2m+1)\ln(0.05)} \sum_{j=i-m}^{i+m} \sum_{x} P_j(\text{residue} = x) \ln P_j(\text{residue} = x)$$

where $P_j(\cdot)$ is the probability of amino acid x appearing at position j and the inner summation is taken over all the amino acids aligned at position j and the values are averaged over a $2m + 1$ residue window centred on residue i (Brown et al., 1993). If all the sequences are identical at position j, then $P_j = 1$ and contributes nothing to M_i, but if two or more amino acids are aligned at position i, then $P_j < 1$ and M_i is increased.

Theoretical structures of the monomers of *Tc*GDH and *Hc*GDH were calculated from amino acid sequences and the structure of *Bt*GDH (1HWY) using Phyre [http://www.sbg.bio.ic.ac.uk/phyre (Kelley & Sternberg, 2009)], ESyPred3D [http://www.fundp.ac.be/sciences/biologie/urbm/bioinfo/esypred (Lambert et al., 2002)] and SWISS-MODEL [http://swissmodel.expasy.org (Kiefer et al., 2009)]. For comparison, a structure of *Tc*GDH based on the *P. falciparum* structure (2BMA) was built using SWISS-MODEL. The quality of fit parameters were calculated using PDBeFold (Krissinel, 2007), which reports three specific scores:

1. The Q score measures the quality of the alignment of the C□s and is calculated from the alignment length (N_{align}) compared with the number of residues in the two amino acid sequences considered (N_1 and N_2) and the root mean square deviation (RMSD) between the C_αs

$$Q = \frac{N_{\text{align}}^2}{\left(1 + (\text{RMSD}/R_0)^2\right) N_1 N_2}$$

where R_0 is empirically set to 3 Å. The value of Q ranges from 1 for identical structures downwards as RMSD rises and N_{align} falls.

2. The P score measures the probability (p) of achieving the same or better quality of match by randomly picking structures from the database

$$P = -\log p$$

so the higher P, the more significant the match.

3. The Z score measures the probability (p_z) that a match of at least the same quality could be obtained by randomly picking structures from the database assuming a normal distribution so

$$p_z = \text{erfc}\left(\frac{Z}{2}\right).$$

If two structures are matched uniquely, then $p_z = p$. The higher Z-score, the higher is the statistical significance of the match.

The residues involved in ligating the reactants or effectors were identified from the relevant *Bt*GDH crystal structures (1HWY, 1HWZ and 3MW9) using PDBsum [http://www.ebi.ac.uk/pdbsum (Laskowski, 2009)]. In each case all residues identified are given even if some are not identified in all the structures. Structural and functional domains were identified using CATH [http://www.cathdb.info (Cuff et al., 2011)] and SCOP [http://scop.mrc-lmb.cam.ac.uk/scop/index.html (Andreeva et al., 2008)].

Figures showing molecular structures were generated using PyMOL [http://sourceforge.net/projects/pymol/].

Results and Discussion

Sequence analysis

A preliminary analysis of the available sequences included GDH sequences from a range of mammals, parasites and microorganisms. Based on this and the available crystal structures, we selected thirteen representative sequences to construct the phylogenetic tree shown in Figure 1. The nematode sequences are clustered together and are clearly distinct from the cluster of protozoan sequences. While there is argument concerning the interpretation of bootstrap probabilities (Soltis & Soltis, 2003), it is clear that the protozoan sequences form a group that is significantly distinct from the nematode and mammalian sequences (Felsenstein & Kishino, 1993; Hillis & Bull, 1993). However, the bovine and human sequences, which have 95% identity (Table 1), are clustered with the nematode sequences (Figure 1). For clarity, we have not included the three protozoan GDHs in the sequence alignment shown in Figure 2. We have also omitted from this analysis the sequence of the sheep GDH (NP_001265496.1) which differs in only 7 positions over the length of the sequence of the bovine enzyme (86% identity, 88% similarity).

RESEARCH ARTICLE

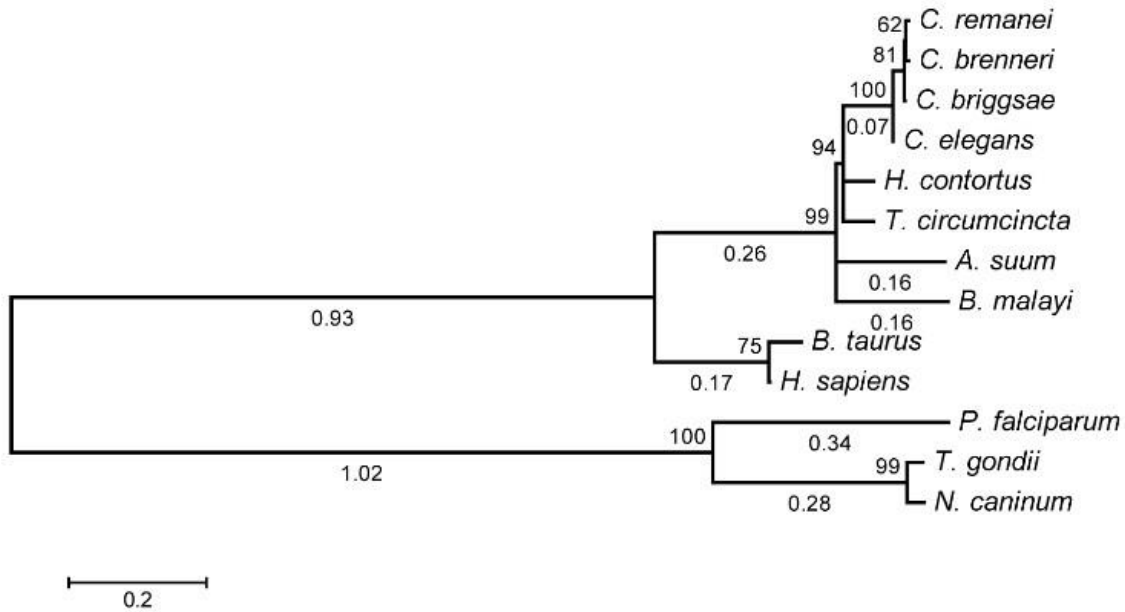

Figure 1. *The bootstrap consensus phylogram derived by maximum likelihood from an alignment of 13 GDH amino acid sequences (432 gap-free positions). The maximum likelihood was based on the JTT matrix-based model (Jones et al., 1992) using 500 bootstrap replicates (Felsenstein, 1985). The percentage of replicate trees in which the associated taxa clustered together in the bootstrap test (500 replicates) are shown as integers next to the branch points. The branch lengths (number of substitutions per site) are indicated below the branches unless the value was less than 0.05 in which case it is not shown. This analysis was conducted using MEGA5 (Tamura et al., 2011).*

Table 1. *Conservation of the amino acid sequence alignment shown in Figure 2. The values are the identity (upper triangle) or the similarity (lower triangle) expressed as a percentage and they were calculated using Clustal X (Thompson et al., 1997).*

	Identity (upper triangle) or similarity (lower triangle) (%)									
	B. malayi	*C. briggsae*	*C. remanei*	*C. brenneri*	*C. elegans*	*A. suum*	*H. contortus*	*T. circumcincta*	*H. sapiens*	*B. taurus*
B. malayi		72	68	71	72	75	72	71	58	57
C. briggsae	86		93	99	97	75	85	86	58	58
C. remanei	81	93		92	91	70	79	80	55	54
C. brenneri	86	99	93		97	75	84	85	58	58
C. elegans	86	99	93	99		75	84	84	58	58
A. suum	87	88	83	88	89		75	75	59	57
H. contortus	85	92	86	91	91	86		91	60	59
T. circumcincta	85	93	87	93	93	87	96		59	59
H. sapiens	74	74	69	74	74	75	74	74		95
B. taurus	73	73	68	73	73	75	73	73	97	

RESEARCH ARTICLE

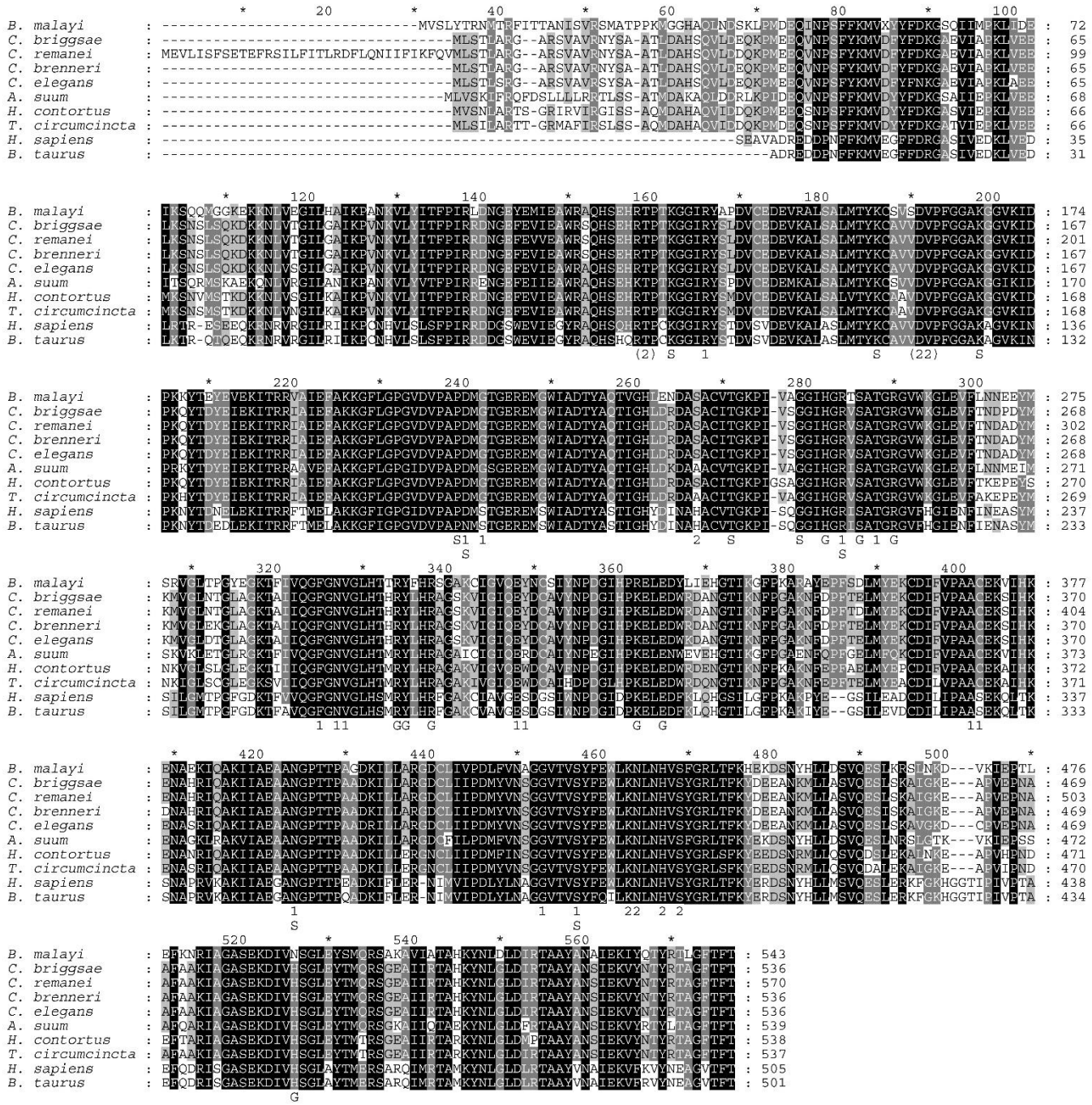

Figure 2. *Alignment of nematode, bovine and human GDH amino acid sequences. The sequences were aligned with Clustal X (Thompson et al., 1997) using the Gonnet matrix, a gap opening penalty of 10 and a gap extension of 0.2. The letters below the alignment indicate the positions of residues involved in ligand binding in the crystal structures (1HWY, 1HWZ and 3MW9) of the bovine enzyme (S – α-ketoglutarate or glutamate; G – GTP; 1 – NAD_a or NADP; 2 – NAD_b; symbols in brackets indicate residues in other subunits).*

RESEARCH ARTICLE

As mentioned previously, the cDNA sequence of GDH from nematodes is very similar to that of mammals (Muhamad et al., 2011). From Figure 2 it is clear that the amino acid sequences are not only highly conserved among nematodes (68-99% identity), but they are also very similar (54-60% identity) to the bovine and human sequences (Table 1).

An interesting feature of the sequence alignment shown in Figure 2 is that *Hc*GDH appears to have a glycine (G240, using the numbering for the *H. contortus* sequence) that is absent from all of the other sequences shown (position 276 of the alignment). This residue forms part of a tripeptide that is relatively poorly conserved between two relatively extensive regions of highly conserved sequence.

Structural models

The human GDH and *Bt*GDH differ very little (Figures 1 and 2) and that other considerations would determine which of them should be used as a basis for the construction of a theoretical model of the *Tc*GDH and *Hc*GDH monomers. Consequently, the availability of kinetic data and several different crystal structures persuaded us to employ *Bt*GDH.

The essential properties of *Bt*GDH are summarised in Figure 3. The glu-binding domain consists of a helical hairpin and a 3-layer(aba) sandwich (structural domains 1 and 2, respectively, in Figure 3) and the NAD-binding domain is a Rossmann fold with an internal region that forms the antenna domain (the stippled region in structural domain 3, Figure 3). Based on the PDBsum analysis of the *Bt*GDH structures, residues involved in binding glutamate and α-ketoglutarate are mostly located in domain 2, but residues in domain 3 are also involved. Similarly, NAD(P) (NAD_a and NADP) binding in the cleft between the glu- and NAD-binding domains involves residues from both domains 2 and 3, although most of the ligands are located in domain 3. Of particular note is R211 in *Bt*GDH that is involved in binding both glutamate/α-ketoglutarate and NAD(P)(H). A second NAD-binding site (NAD_b) involves other residues in domains 2 and 3, as well as three residues in domain 2 of an adjacent subunit. Most of the residues involved in GTP binding are located in domain 3. All of these residues are located in relatively well conserved regions of the sequence and both the N-terminal portion of the NAD-binding domain and the antenna domain are relatively poorly conserved (Figure 3).

Of all the residues involved in binding NAD(P), α-ketoglutarate, glutamate or GTP, only six in *Bt*GDH (N168, S170, H195, S276, S327, D388) differ from the corresponding residues in *Tc*GDH (D, G, A, W, C, N) or *Hc*GDH (D, G, S, W, C, N), as shown in Figures 2 and 3. Of these, two (H195 ↔ A/S and D388 ↔ N) ligate NAD_b and will not be considered further, and another three are relatively conservative substitutions (N168 ↔ D, S170 ↔ G, S327 ↔ C). The sixth difference (S276 ↔ W) is more significant because a small polar residue (S) is replaced with a larger hydrophobic residue (W), but it is especially interesting as S276 in *Bt*GDH (1HWZ) ligates the 2′-phosphate of NADP(H).

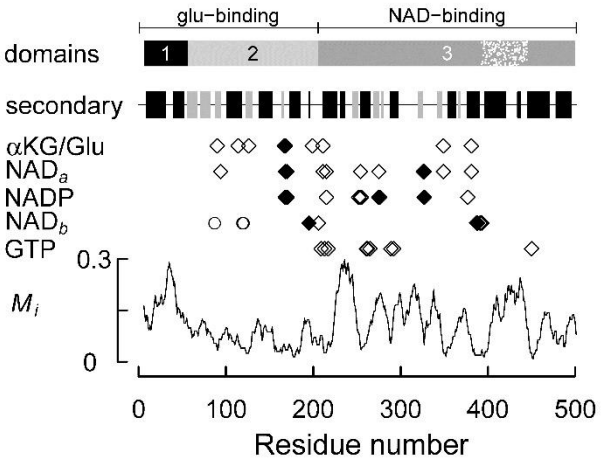

Figure 3. *Summary of the structure and ligand binding sites of BtGDH and sequence mutability (M_i) of selected GDHs. The symbols (◊, ♦, ○) indicate residues that are hydrogen bonded to the substrate, cofactor or effector. The residues at positions 87, 119 and 120, indicated by open circles (○), are located in another subunit. Those residues indicated by solid diamonds (♦) differ between BtGDH and TcGDH or HcGDH. The three structural domains (1-3) were identified using CATH (http://www.cathdb.info (Cuff et al., 2011)) and the two functional domains were identified using SCOP [http://scop.mrc-lmb.cam.ac.uk/scop/index.html (Andreeva et al., 2008)]. The stippled region in domain 3 represents the 'antenna' domain. The secondary structure indicates the positions of α-helices and β-strands (black and grey rectangles, respectively).*

Three model structures were constructed for each of the *Tc*GDH and *Hc*GDH amino acid sequences. In each case, the models had the glu- and NAD-binding domains, as well as the antenna domain like *Bt*GDH (Figure 4), but unlike the *P. falciparum* GDH (2BMA, (Werner et al., 2005)) and the bacterial enzyme (Peterson & Smith, 1999).

RESEARCH ARTICLE

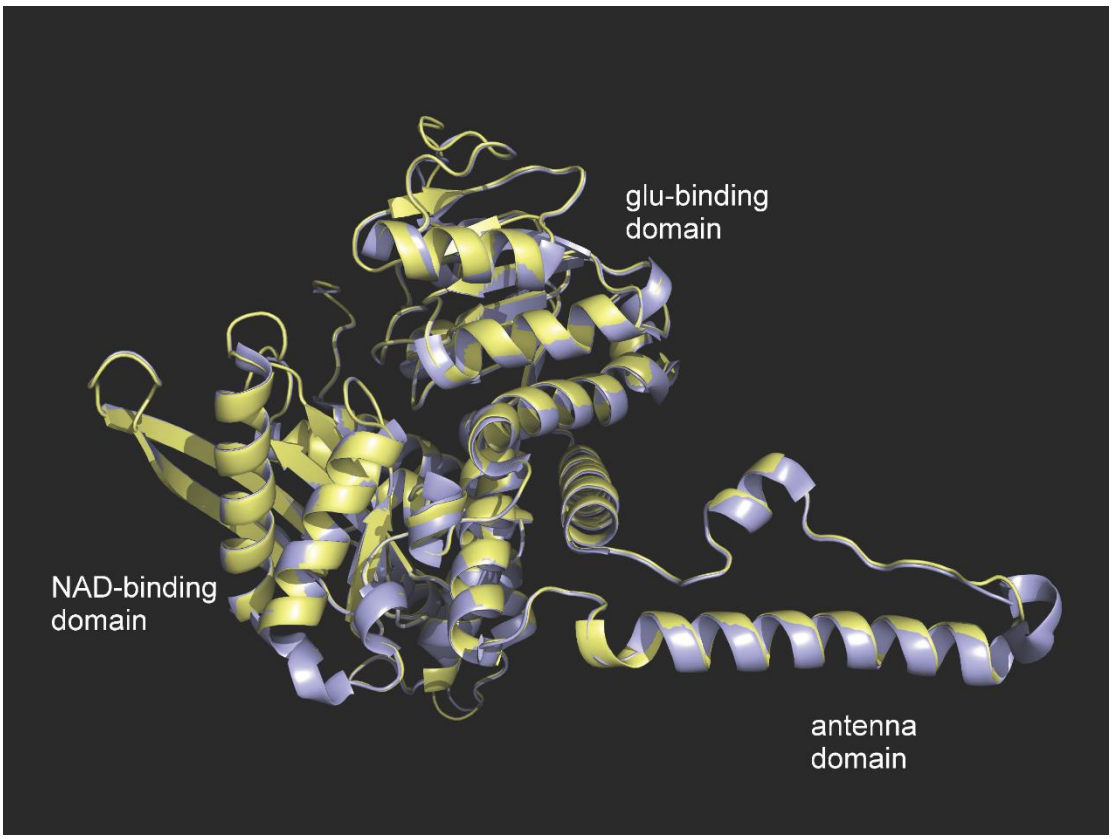

Figure 4. *Superimposition of BtGDH (1HWY in blue) and the model of TcGDH generated using SWISS-MODEL (in yellow).*

Table 2. *Quality of fit parameters for predicted structures obtained for the T. circumcincta and H. contortus sequences (AEO44571.1 and AAC19750.1, respectively) based on the BtGDH structure (1HWY). Structures were calculated using Phyre (Kelley & Sternberg, 2009), ESyPred3D (Lambert et al., 2002) and SWISS-MODEL (Kiefer et al., 2009) and the quality of fit parameters were calculated using PDBeFold (Krissinel, 2007).*

	Phyre	ESyPred3D	SWISS-MODEL
T. circumcincta			
Q	0.5529	0.8863	0.9698
P	23.97	54.23	81.84
Z	15.34	22.26	27.34
RMSD (Å)	2.001	0.551	0.364
Number of residues aligned	446	480	497
Identical residues aligned (%)	58.74	65	63.78
H. contortus			
Q	0.5542	0.8757	0.9753
P	22.92	54.58	77.77
Z	14.78	22.33	26.72
RMSD (Å)	2.016	0.404	0.251
Number of residues aligned	448	474	497
Identical residues aligned (%)	58.04	64.56	64.19

RESEARCH ARTICLE

While all these structures were similar, those generated using SWISS-MODEL appeared to be the best (Table 2) because they had the smallest root mean square deviation (RMSD) from 1HWY, and the largest quality measures (*Q*, *P* and *Z*). For comparison, a theoretical structure of the *Tc*GDH monomer based on the *P. falciparum* structure (2BMA) was built using SWISS-MODEL and this was clearly inferior (*Q* = 0.7618, *P* = 57.99, *Z* = 24.05, RMSD = 0.513 Å) to those based on the *Bt*GDH structure (Table 2). Moreover, the models based on *Bt*GDH yielded Ramachandran plots that were very similar to that of the bovine enzyme (Figure 5, A and B). This indicates that the backbone dihedral angles had not been greatly distorted in the model, which can be confirmed by inspection of Figure 4 in which the backbones of the aligned *Bt*GDH and model *T. circumcincta* structures are supermposed. Naturally, there is rather more variation in the positions of the side chains, but those residues involved in ligand binding are largely in very similar positions even where the residues differ (Figure 6). The most significant exception to this generalisation is S276, which is located adjacent to the adenine ring of $NAD(P)^+$ and provides three H-bonds to the 2′-phosphate of $NADP^+$ in *Bt*GDH (1HWZ). In the model *Tc*GDH and *Hc*GDH structures S276 is replaced with a tryptophan, the sidechain of which lies outside the electron density of the serine sidechain (Figure 6). This difference involves the replacement of the polar sidechain with a hydrophobic sidechain that is significantly larger, resulting in the partial occlusion of the NAD(P)-binding site and removal of at least one potential H-bond to the 2′-phosphate group.

The glycine residue that appears to be specific to *Hc*GDH (G240) forms part of a loop that is distinct from the corresponding helix fragments found in *Tc*GDH and *Bt*GDH (indicated by G in Figure 7). This loop is exposed at the surface of the structure and is adjacent to the α-ketoglutarate/glu-binding site (indicated by S in Figure 7) and is located in the vicinity of three ligands (Figure 2). In Figure 7 it is clear that the α-ketoglutarate is parallel to a helix that is essentially identical in *Bt*GDH and the model structures of *Tc*GDH and *Hc*GDH. The other side of the binding site is formed by loops that appear to protude further into the site in the model *Tc*GDH and *Hc*GDH structures than in the *Bt*GDH structure (indicated by the three asterisks in Figure 7). The residues directly involved in binding α-ketoglutarate or glutamate, based on the PDBsum analysis, are essentially identical in all three structures except for N168, which is replaced with an aspartate in both nematode sequences (Figure 2). It is clear from Figure 8 that the orientation of the sidechain differs between the *Bt*GDH and the model structures and that this results in the loss of an H-bond.

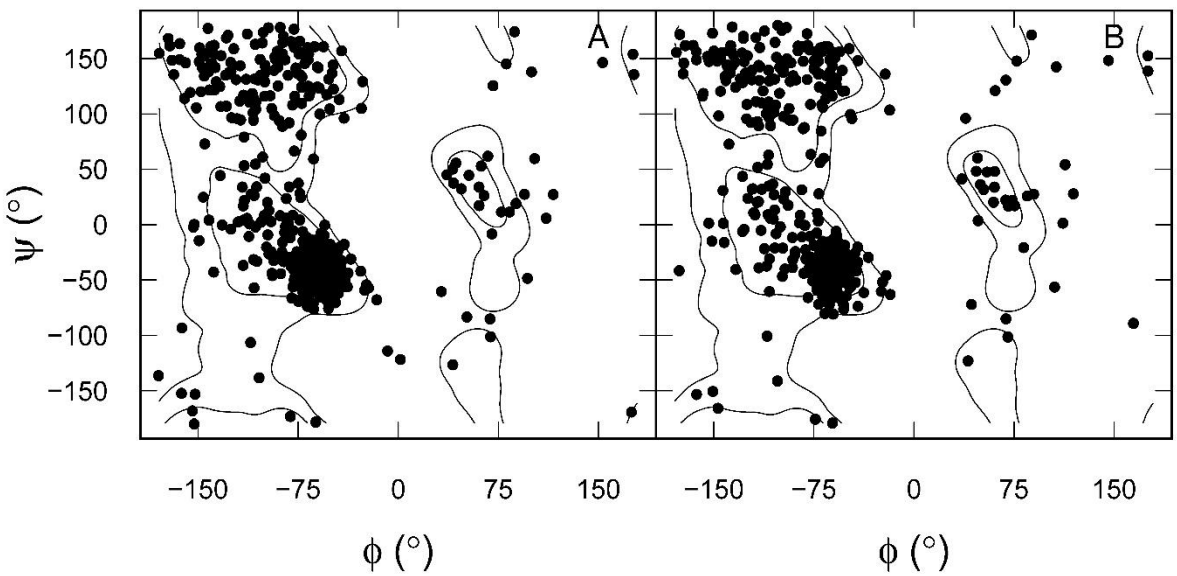

Figure 5. *Ramachandran plots for BtGDH (A, 1HWY) and SWISS-MODEL derived TcGDH (B) structures. The contours are based on those of Lovell et al. (2003).*

RESEARCH ARTICLE

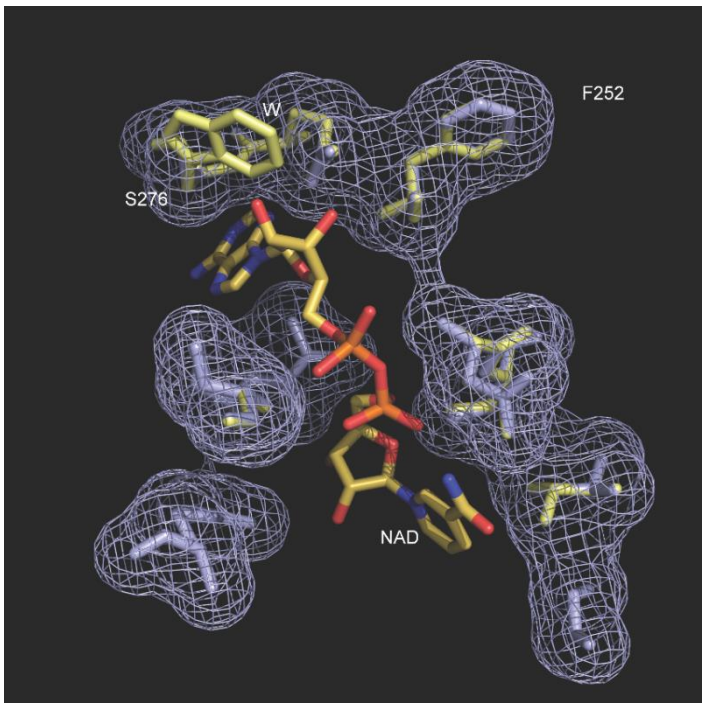

Figure 6. *Structural alignment showing the NAD(P)-binding residues of BtGDH (1HWY, in blue) and the corresponding residues in the model of TcGDH generated using SWISS-MODEL (yellow). Also shown is the NAD$^+$ bound in the BtGDH structure. Note that the tryptophan corresponding to S276 in BtGDH is very close to the 2'-OH of NAD$^+$ and that the tryptophan side-chain lies outside the electron density of S276.*

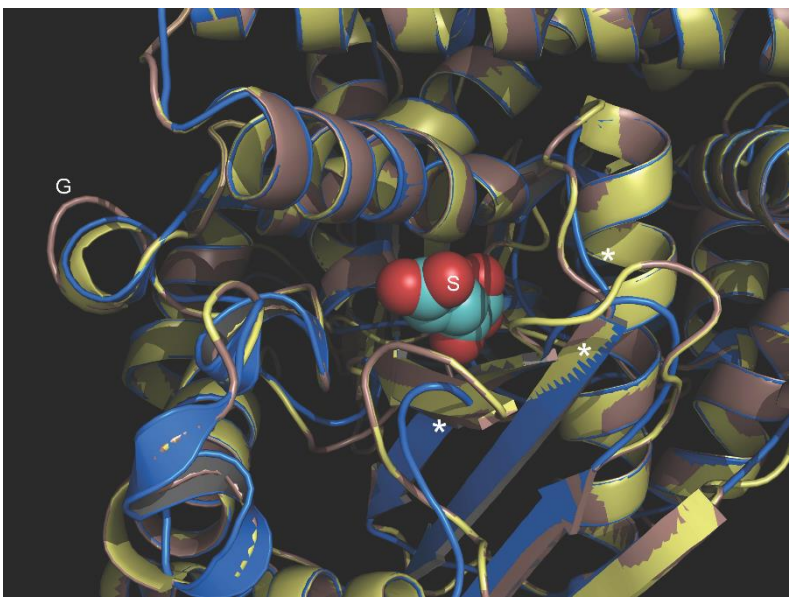

Figure 7. *The structure of the α-ketoglutarate/glu-binding site in BtGDH (1HWY, blue) and in the model TcGDH (yellow) and HcGDH (red) structures. The bovine structure has α-ketoglutarate bound at this site (S) and G240 in the HcGDH sequence (G) and the three loops (*) that protrude more into the binding site in the model stuctures than in BtGDH are also indicated (towards the lower right of the α-ketoglutarate).*

RESEARCH ARTICLE

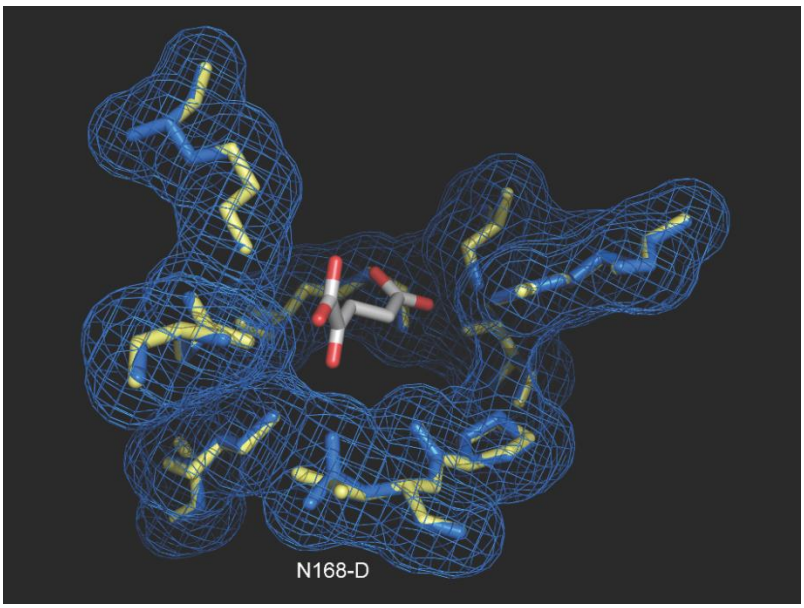

Figure 8. *Details of the ligands forming the α-ketoglutarate/glu-binding site in BtGDH (1HWY, blue) and in the model TcGDH (yellow).*

Structural implications

Both the structural and kinetic properties of *Tc*GDH and *Hc*GDH are more like those of the bovine enzyme than those of the *P. falciparum* GDH. The ligand binding residues are similar and the backbone of the monomer is not distorted relative to the bovine enzyme. However, six residues involved in ligating substrates or cofactors differ between *Bt*GDH and *Tc*GDH (Figures 2 and 3). The K_m for NAD(P)H is about 0.02 mM for the bovine enzyme (Rife & Cleland, 1980; McCarthy & Tipton, 1985) and only very slightly larger (0.03-0.05 mM) for rGDH and *Hc*GDH (Rhodes & Ferguson, 1973; Umair et al., 2011).

The most significant kinetic difference between *Bt*GDH and the *Tc*GDH is the K_m for $NADP^+$ (Table 3). This has been reported to be 0.028 mM for the bovine enzyme (Rife & Cleland, 1980; McCarthy & Tipton, 1985) and 1 mM for *Tc*GDH (Umair et al., 2011). The 2′-phosphate group of $NADP^+$ is ligated by S276 in the bovine enzyme, but this is replaced by a tryptophan in r*Tc*GDH (Figure 1A). This has two effects: (a) the terminal hydroxyl group is absent from the side chain, removing one possible H-bond and (b) there is less space available for the $NADP^+$. It might be speculated that the steric constraint is especially likely to provide some rationalisation for the lower affinity of *Tc*GDH for $NADP^+$, which might also explain the small decrease in the affinity of *Tc*GDH for NAD(H). Some limited support for this speculation is provided by a report (Yoon et al., 2002) with human GDH mutants of a residue equivalent to E275, in each of which the K_m(NADH) was increased about 10-fold. Unfortunately, the similarity between *Tc*GDH and *Hc*GDH means that only one ligand binding residue is different (H195 is replaced with S rather than A). This does not explain the lack of activity of *Hc*GDH with NADP(H) (Rhodes & Ferguson, 1973).

A less significant difference in the reported kinetics of the three enzymes is that K_m(glutamate) and K_m(α-ketoglutarate) are much smaller in *Tc*GDH than in *Hc*GDH (Table 3). While this might relate to the assay conditions, the model structures of the binding site shown in Figure 7 prompt the speculation that the extra residue in *Hc*GDH (G240) might make the loop in which it is located more flexible than the corresponding helix-fragments in *Bt*GDH and the model *Tc*GDH. Perhaps this possible flexibility makes access to the site slightly more difficult. In contrast, the corresponding K_ms of *Tc*GDH are smaller than those reported for *Bt*GDH (Table 3). This could relate to the loops that protude into the site more in *Tc*GDH (and *Hc*GDH) than they do in *Bt*GDH (Figure 7). If this is the case, then the larger K_m(glutamate) and K_m(α-ketoglutarate) of *Hc*GDH are even more significant.

RESEARCH ARTICLE

Table 3. *Values of the K_ms reported for BtGDH, r TcGDH, TcGDH and HcGDH.*

	K_m (mM)			
	Bos taurus[a]	*T. circumcincta*		*H. contortus*[d]
		r*Tc*GDH[b]	*Tc*GDH[c]	
α-ketoglutarate	0.36-2.4	0.07-0.1	0.06-0.09	0.74
glutamate	0.74-3	0.35-0.45	0.15-0.7	3.3
NAD^+	0.076-0.22	0.7	0.7	0.31
$NADP^+$	0.028	1	3	—
NADH	0.02	0.05	0.025	0.033
NADPH	0.02-0.022	0.03	0.10	—
NH_3	6.5-50	37-40	18	42

[a] (Frieden, 1959; Engel & Dalziel, 1969; Rife & Cleland, 1980; McCarthy & Tipton, 1985) [b] (Umair et al., 2011) [c] (Muhamad et al., 2011)
[d] (Rhodes & Ferguson, 1973)

Conclusion

It has been suggested that GDH is a potential target for anthelmintics (Umair et al., 2011) because there are "significant differences" in amino acid sequence between the host and the parasite enzyme. The structural models of *Tc*GDH and *Hc*GDH described here were based on the bovine enzyme, which differs in only 7 positions from the sequence of the sheep enzyme. We infer from this conservation of sequence (Figure 2) and, consequently, of model structure (Figure 4) that the "significant differences" to which Umair et al. (2011) refer, but do not define, are unlikely to render the parasite GDHs sufficiently different from that of the host to make them viable therapeutic targets. However, the replacement of S276 with a tryptophan in the nematode GDHs (Figure 6) provides a plausible explanation of their reduced affinity for $NADP^+$ (Table 3) and this may have significant implications for amino acid metabolism.

References

Andreeva A, Howorth D, Chandonia J-M, Brenner SE, Hubbard TJP, Chothia C, Murzin AG. 2008. Data growth and its impact on the SCOP database: new developments. Nucleic Acids Res., 36(Database issue)**:**D419-D425.

Brown S, Moody AJ, Mitchell R, Rich PR. 1993. Binuclear centre structure of terminal protonmotive oxidases. FEBS Lett., 316(3)**:**216-223.

Cuff AL, Sillitoe I, Lewis T, Clegg AB, Rentzsch R, Furnham N, Pellegrini-Calance M, Jones D, Thornton J, Orengo CA. 2011. Extending CATH: increasing coverage of the protein structure universe and linking structure with function. Nucleic Acids Res., 39(Database issue)**:**D420-D426.

Engel PC, Dalziel K. 1969. Kinetic studies of glutamate dehydrogenase with glutamate and norvaline as substrates. Coenzyme activation and negative homotropic interactions in allosteric enzymes. Biochem. J., 115(4)**:**621-631.

Felsenstein J. 1985. Confidence limits on phylogenies: an approach using the bootstrap. Evolution, 39(4)**:**783-793.

Felsenstein J, Kishino H. 1993. Is there something wrong with the bootstrap on phylogenies? A reply to Hillis and Bull. Syst. Biol., 42(2)**:**193-200.

Frieden C. 1959. Glutamic dehydrogenase. III. The order of substrate addition in the enzymatic reaction. J. Biol. Chem., 234(11)**:**2891-2896.

Frigerio F, Casimir M, Carobbio S, Maechler P. 2008. Tissue specificity of mitochondrial glutamate pathways and the control of metabolic homeostasis. Biochim. Biophys. Acta, 1777(7-8)**:**965-972.

Gore MG. 1981. L-glutamic acid dehydrogenase. Int. J. Biochem., 13(8)**:**879-886.

Green L, Simcock DC, Muhamad N, Page R, Patchett ML, Simpson HV, Brown S. 2004. Molecular properties of two dehydrogenases active in L_3 *Ostertagia circumcincta*. N. Z. J. Zool., 31(4)**:**376-377.

Hillis DM, Bull JJ. 1993. An empirical test of bootstrapping as a method for assessing confidence in phylogenetic analysis. Syst. Biol., 42(2)**:**182-192.

Hudson RC, Daniel RM. 1993. L-Glutamate dehydrogenases: distribution, properties and mechanism. Comp. Biochem. Physiol., 106B(4)**:**767-792.

Jones DT, Taylor WR, Thornton JM. 1992. The rapid generation of mutation data matrices from protein sequences. CABIOS, 8(3)**:**275-282.

Kelley LA, Sternberg MJE. 2009. Protein stucture prediction on the web: a case study using the Phyre server. Nature Protocols, 4(3)**:**363-371.

Kiefer F, Arnold K, Künzli M, Bordoli L, Schwede T. 2009. The SWISS-MODEL repository and associated resources. Nucleic Acids Res., 37(Database issue)**:**D387-D392.

Kim DW, Eum WS, Jang SH, Yoon CS, Kim YH, Choi SH, Choi HS, Kim SY, Kwon HY, Kang JH, Kwon O-S, Cho S-W, Park J, Choi SY. 2003. Molecular gene cloning, expression, and characterization of bovine brain glutamate dehydrogenase. J. Biochem. Mol. Biol., 36(6)**:**545-551.

RESEARCH ARTICLE

Krissinel E. 2007. On the relationship between sequence and structure similarities in proteomics. Bioinform., 23(6)**:**717-723.

Lambert C, Léonard N, De Bolle X, Depiereux E. 2002. ESyPred3D: prediction of proteins 3D structures. Bioinform., 18(9)**:**1250-1256.

Laskowski RA. 2009. PDBsum new things. Nucleic Acids Res., 37(Database issue)**:**D355-D359.

Lovell SC, Davis IW, Arendall WB, III, de Bakker PIW, Word JM, Prisant MG, Richardson JS, Richardson DC. 2003. Structure validation by Ca geometry: f, y and Cb deviation. Proteins, 50(3)**:**437-450.

Marzluf GA. 1981. Regulation of nitrogen metabolism and gene expression in fungi. Microbiol. Revs., 45(3)**:**437-461.

Mayashita Y, Good AG. 2008. Glutamate deamination by glutamate dehydrogenase plays a central role in amino acid catabolism in plants. Plant Signal. Behavior, 3(10)**:**842-843.

McCarthy AD, Tipton KF. 1985. Ox glutamate dehydrogenase. Comparison of the kinetic properties of native and proteolysed preparations. Biochem. J., 230(1)**:**95-99.

Muhamad N, Simcock DC, Pedley KC, Simpson HV, Brown S. 2011. The kinetics of glutamate dehydrogenase of *Teladorsagia circumcincta* and the lifestyle of the parasite. Comp. Biochem. Physiol., 159B(2)**:**71-77.

Newsholme P, Lima MMR, Procopio J, Pithon-Curi TC, Doi SQ, Bazotte RB, Curi R. 2003. Glutamine and glutamate as vital metabolites. Braz. J. Med. Biol. Res., 36(2)**:**153-163.

Owen OE, Kalhan SC, Hanson RW. 2002. The key role of anaplerosis and cataplerosis for citric acid cycle function. J. Biol. Chem., 277(34)**:**30409-30412.

Peterson PE, Smith TJ. 1999. The structure of bovine glutamate dehydrogenase provides insights into the mechanism of allostery. Structure, 7(7)**:**769-782.

Plaitakis A, Zaganas I. 2001. Regulation of human glutamate dehydrogenases: implications for glutamate, ammonia and energy metabolism in brain. J. Neurosci. Res., 66(5)**:**899-908.

Rhodes MB, Ferguson DL. 1973. Haemonchus contortus: enzymes. III. Glutamate dehydrogenase. Exptl. Parasitol., 34(1)**:**100-110.

Rife JE, Cleland WW. 1980. Kinetic mechanism of glutamate dehydrogenase. Biochem., 19(11)**:**2321-2328.

Skuce PJ, Stewart EM, Smith WD, Knox DP. 1999. Cloning and characterization of glutamate dehydrogenase (GDH) from the gut of *Haemonchus contortus*. Parasitol., 118(3)**:**297-304.

Soltis PS, Soltis DE. 2003. Applying the bootstrap in phylogeny reconstruction. Statist. Sci., 18(2)**:**256-267.

Storm J, Perner J, Aparicio I, Patzewitz E-M, Olszewski K, Llinas M, Engel PC, Müller S. 2011. *Plasmodium falciparum* glutamate dehydrogenase a is dispensable and not a drug target during erythrocytic development. Malaria J., 10:193.

Tamura K, Peterson D, Peterson N, Stecher G, Nei M, Kumar S. 2011. MEGA5: molecular evolutionary genetics analysis using maximum likelihood, evolutionary distance, and maximum parsimony methods. Mol. Biol. Evol., 28(10)**:**2731-2739.

Thompson JD, Gibson TJ, Plewniak F, Jeanmougin F, Higgins DG. 1997. The ClustalX windows interface: flexible strategies for multiple sequence alignment aided by quality analysis tools. Nucleic Acids Res., 25(24)**:**4876-4882.

Umair S, Knight JS, Patchett ML, Bland RJ, Simpson HV. 2011. Molecular and biochemical characterisation of a *Teladorsagia circumcincta* glutamate dehydrogenase. Exptl. Parasitol., 129(3)**:**240-246.

van Wyk JA, Malan FS, Randles JL. 1997. How long before resistance makes it impossible to control some field strains of Haemonchus contortus in South Africa with any of the modern anthelmintics? Vet. Parasitol., 70(1-3)**:**111-122.

Waller PJ, Echevarria F, Eddi C, Maciel S, Nari A, Hansen JW. 1996. The prevalence of anthelmintic resistance in nematode parasites of sheep in Southern Latin America: General overview. Vet. Parasitol., 62(3-4)**:**181-187.

Werner C, Stubbs MT, Krauth-Siegel RL, Klebe G. 2005. The crystal structure of *Plasmodium falciparum* glutamate dehydrogenase, a putative target for novel antimalarial drugs. J. Mol. Biol., 349(3)**:**597-607.

Yoon H-Y, Cho EH, Kwon HY, Choi SY, Cho S-W. 2002. Importance of glutamate 279 for the coenzyme binding of human glutamate dehydrogenase. J. Biol. Chem., 277(44)**:**41448-41454.